Collective Flow signals the Quark Gluon Plasma *

H. Stöcker
Institut für Theoretische Physik, Johann Wolfgang Goethe – Universität, Robert Mayer Str. 8-10, 60054 Frankfurt am Main, Germany and Frankfurt Institute for Advanced Studies (FIAS), Robert Mayer Str. 8-10, 60054 Frankfurt am Main, Germany

A critical discussion of the present status of the CERN experiments on charm dynamics and hadron collective flow is given. We emphasize the importance of the flow excitation function from 1 to 50 A·GeV: here the hydrodynamic model has predicted the collapse of the v_1-flow and of the v_2-flow at ~ 10 A·GeV; at 40 A·GeV it has been recently observed by the NA49 collaboration. Since hadronic rescattering models predict much larger flow than observed at this energy we interpret this observation as potential evidence for a first order phase transition at high baryon density ρ_B. A detailed discussion of the collective flow as a barometer for the equation of state (EoS) of hot dense matter at RHIC follows. Here, hadronic rescattering models can explain $< 30\%$ of the observed elliptic flow, v_2, for $p_T > 2$ GeV/c. This is interpreted as evidence for the production of superdense matter at RHIC with initial pressure far above hadronic pressure, $p > 1$ GeV/fm^3. We suggest that the fluctuations in the flow, v_1 and v_2, should be measured in future since ideal hydrodynamics predicts that they are larger than 50 % due to initial state fluctuations. Furthermore, the QGP coefficient of viscosity may be determined experimentally from the fluctuations observed. The connection of v_2 to jet suppression is examined. It is proven experimentally that the collective flow is not faked by minijet fragmentation. Additionally, detailed transport studies show that the away-side jet suppression can only partially ($< 50\%$) be due to hadronic rescattering. We, finally, propose upgrades and second generation experiments at RHIC which inspect the first order phase transition in the fragmentation region, i.e. at $\mu_B \approx 400$ MeV ($y \approx 4-5$), where the collapse of the proton flow should be seen in analogy to the 40 A·GeV data. The study of Jet-Wake-riding potentials and Bow shocks – caused by jets in the QGP formed at RHIC – can give further information on the equation of state (EoS) and transport coefficients of the Quark Gluon Plasma (QGP).

I. OLD AND NEW OBSERVABLES FOR THE QGP PHASE TRANSITION

Lattice QCD results [1, 2] (cf. Fig. 1) show a crossing, but no first order phase transition to the QGP for vanishing or small chemical potentials μ_B, i.e. at the conditions accessible at central rapidities at RHIC full energies. A first order phase transition does occur according to the QCD lattice calculations [1, 2] only at high baryochemical potentials or densities, i.e. at SIS-300 and lower SPS energies and in the fragmentation region of RHIC, $y \approx 4-5$ [3, 4]. The critical baryochemical potential is predicted [1, 2] to be $\mu_B^c \approx 400 \pm 50$ MeV and the critical temperature $T_c \approx 150-160$ MeV. We do expect a phase transition also at finite strangeness. Predictions for the phase diagram of strongly interacting matter for realistic non-vanishing net strangeness are urgently needed to obtain a comprehensive picture of the QCD phase structure. Multi-Strangeness degrees of freedom are very promising probes for the properties of the dense and hot matter [5]. The strangeness distillation process [6, 7] predicts dynamical de-admixture of s and $\bar{s}$ quarks, which yields unique signatures for QGP creation: high multistrange hyperon-/-matter production, strangelet formation and unusual antibaryon to baryon ratios *ect.*

A. Thermodynamics in the $T - \mu_B$ plane

A comparison of the thermodynamic parameters T and μ_B extracted from the UrQMD-transport model in the central overlap regime of Au+Au collisions [9] with the QCD predictions is shown in Fig 1, where the full dots with errorbars denote the 'experimental' chemical freeze-out parameters – determined from fits to the experimental yields – taken from Ref. [10]. The triangular and quadratic symbols (time-ordered in vertical sequence) stand for temperatures T and chemical potentials μ_B extracted from UrQMD transport calculations in central Au+Au (Pb+Pb) collisions at RHIC (21.3 A·TeV), 160, 40 and 11 A·GeV [8] as a function of the reaction time (separated by 1 fm/c steps from

* Supported by DFG, GSI, BMBF, EU, RIKEN and DOE

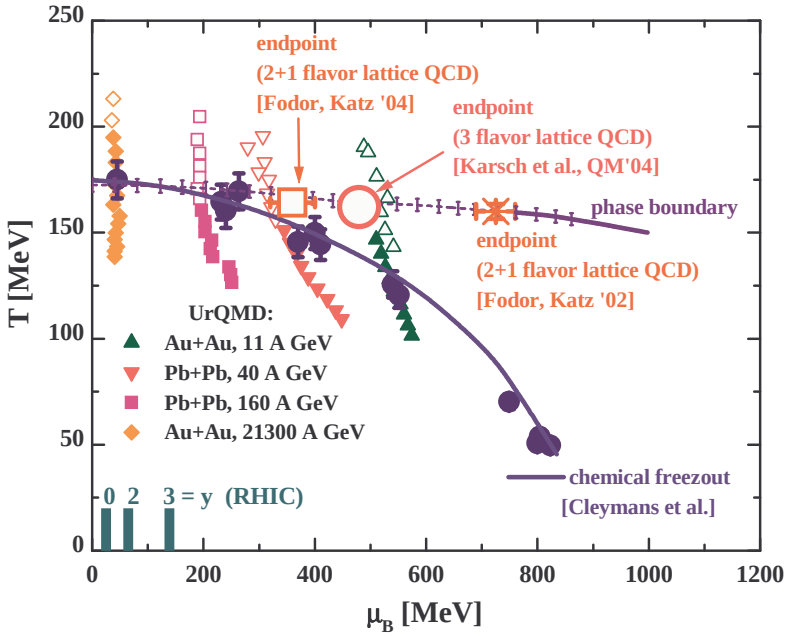

FIG. 1: The new phase diagram with the critical end point at $\mu_B \approx 400$ MeV, $T \approx 160$ MeV as predicted by Lattice QCD. In addition, the time evolution in the $T-\mu$-plane of a central cell in UrQMD calculations [8] is depicted for different bombarding energies. Note, that the calculations indicate that bombarding energies $E_{LAB} \lesssim 40$ A·GeV are needed to probe a first order phase transition. At RHIC (see insert at the μ_B scale) this point is accessible in the fragmentation region only (taken from [9]).

top to bottom). The open symbols denote nonequilibrium configurations and correspond to T parameters extracted from the transverse momentum distributions, whereas the full symbols denote configurations in approximate pressure equilibrium in longitudinal and transverse direction.

During the nonequilibrium phase (open symbols) the transport calculations show much higher temperatures (or energy densities) than the 'experimental' chemical freeze-out configurations at all bombarding energies (≥ 11 A·GeV). These numbers are also higher than the critical point (circle) of (2+1) flavor - Lattice QCD calculations by the Bielefeld-Swansea-collaboration [2] (large open circle) and by the Wuppertal-Budapest-collaboration [1] (the star shows earlier results from [1]). The energy density at μ_c, T_c is in the order of ≈ 1 GeV/fm^3 (or slightly below). At RHIC energies a cross-over is expected at midrapidity, when stepping down in temperature during the expansion phase of the 'hot fireball'. The baryon chemical potential μ_B for different rapidity intervals at RHIC energies has been obtained from a statistical model analysis by the BRAHMS Collaboration based on measured antihadron to hadron yield ratios [11]. For midrapidity one finds $\mu_B \simeq 0$, whereas for forward rapidities μ_B increases up to $\mu_B \simeq 130$ MeV at $y = 3$. Thus, only extended forward rapidity measurement ($y \approx 4-5$) will allow to probe large μ_B at RHIC. The detectors at RHIC at present offer only a limited chemical potential range. To reach the first order phase transition region at midrapidity, the International Facility at GSI seems to be the right place to go. This situation changes at lower SPS (and top AGS) as well as at the future GSI SIS-300 energies: sufficiently large chemical potentials μ_B should allow for a first order phase transition [12] (to the right of the critical point in the (T, μ_B) plane). The transport calculations show high temperatures (high energy densities) in the very early phase of the collisions, only. Here, hadronic interactions are weak due to formation time effects and yield little pressure. Diquark, quark and gluon interactions should cure this problem.

B. Open charm and charmonia at SPS and RHIC

Open charm and charmonium production at SPS and RHIC energies has been calculated within the HSD and UrQMD transport approaches [13] using parametrizations for the elementary production channels including the charmed hadrons $D, \bar{D}, D^*, \bar{D}^*, D_s, \bar{D}_s, D_s^*, \bar{D}_s^*$, $J/\Psi, \Psi(2S), \chi_{2c}$ from NN and πN collisions. The latter parametrizations are fitted to PYTHIA calculations [14] above $\sqrt{s} = 10$ GeV and extrapolated to the individual thresholds, while the absolute strength of the cross sections is fixed by the experimental data as described in Ref. [15]; for previous

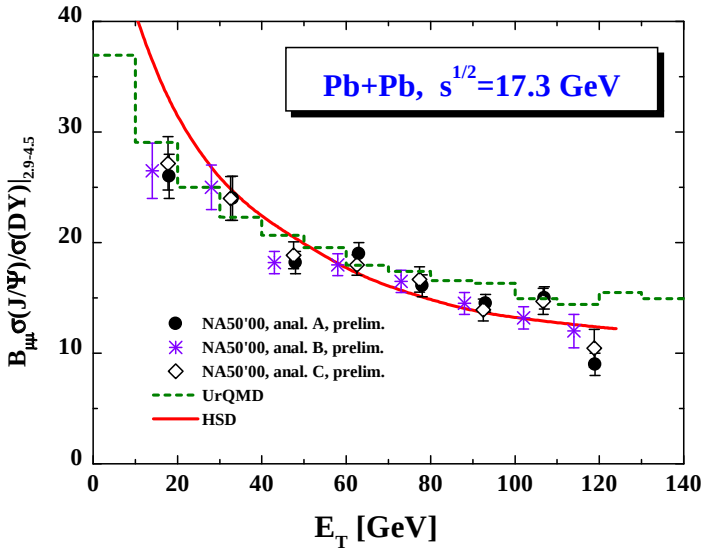

FIG. 2: The J/Ψ suppression as a function of the transverse energy E_T in $Pb + Pb$ collisions at 160 A·GeV. The solid line shows the HSD result within the comover absorption scenario [19]. The different symbols stand for the NA50 data [20] from the year 2000 (analysis A,B,C) while the dashed histogram is the UrQMD result [18].

works see [16, 17, 18] Backward channels 'charm + anticharm meson → charmonia + meson' are treated via detailed balance in a more schematic interaction model with a single parameter or matrix element $|M|^2$ that is fixed by the J/Ψ suppression data from the NA50 collaboration at SPS energies (cf. Ref. [19]).

We recall that charmonium suppression had been proposed as "the clearest" QGP-signature and the community has been riding on this folklore for almost two decades. Hence, these detailed comparisons come as a shock: The $Pb + Pb$ results at 160 A·GeV, both from UrQMD and HSD transport calculations are well in line with the data of the NA50 Collaboration in Fig. 2, where the J/Ψ suppression is shown as a function of the transverse energy E_T. The solid line stands for the HSD result within the comover absorption scenario while the various data points reflect the NA50 data from the year 2000 (analysis A,B,C). The data have moved so that they agree now with the HSD and UrQMD calculations [18] (dashed histogram in Fig. 2). We mention that there might be alternative explanations

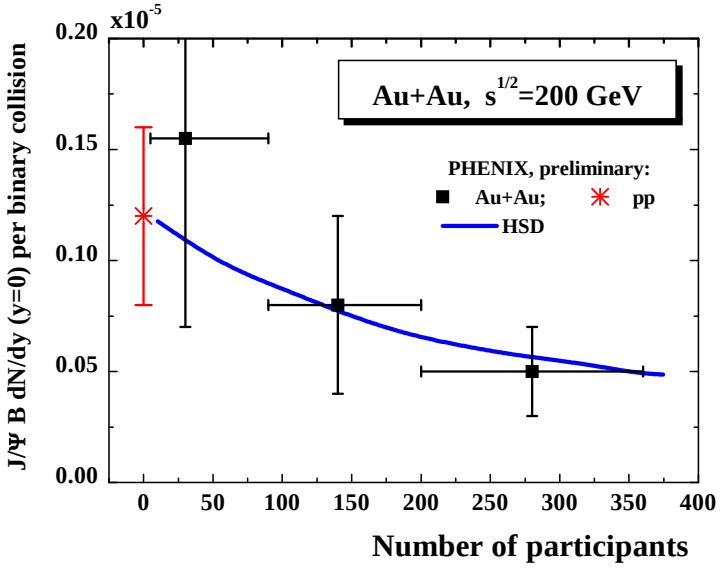

FIG. 3: The calculated J/Ψ multiplicity per binary collision – multiplied by the branching to dileptons – as a function of the number of participating nucleons, N_{part}, in comparison to the preliminary data from the PHENIX collaboration [23] for $Au + Au$ and pp reactions (taken from Ref. [19]).

for J/Ψ suppression, as discussed in Refs. [21, 22] and/or further (dissociation) mechanisms not considered here. However, for the purposes of the present review it is sufficient to point out that

a) no sign of unusual physics can be related to the J/Ψ data and

b) the models employed here (cf. Figs. 6 and 7 in [19]) use upper limits for the dissociation cross sections and do not lead to a sizeable re-creation of charmonia by $D + \bar{D}$ channels at SPS energies.

At RHIC central $Au + Au$ collisions at $\sqrt{s} = 200$ GeV will, however, produce multiplicities of open charm pairs about 2 orders of magnitude larger than at 160 A·GeV, such that a much higher J/Ψ reformation rate ($\sim N_{c\bar{c}}^2$) is expected (cf. Ref. [22]). At RHIC top energy, $\sqrt{s} = 200$ GeV, the J/Ψ comover dissociation may no longer be important, since the charmonia dissociated in this channel are approximately recreated in the backward channels. Hence, the J/Ψ dissociation at RHIC should be less pronounced than at SPS energies.

The preliminary data of the PHENIX Collaboration [23] allow for a first glance at the situation encountered in $Au + Au$ collisions at $\sqrt{s} = 200$ GeV. Fig. 3 shows the J/Ψ multiplicity per binary collision as a function of the number of participating nucleons N_{part} in comparison to the data at midrapidity. The statistics is quite limited; thus no final conclusion can presently be drawn. However, the data neither suggest a dramatic enhancement of J/Ψ production nor a complete 'melting' of the charmonia in the QGP phase.

C. Historical Interlude

Hydrodynamic flow and shock formation has been proposed early [24, 25] as the key mechanism for the creation of hot and dense matter during relativistic heavy-ion collisions. The full three-dimensional hydrodynamical flow problem is much more complicated than the one-dimensional Landau model [26]: the 3-dimensional compression and expansion dynamics yields complex triple differential cross-sections, which provide quite accurate spectroscopic handles on the equation of state. The bounce-off, $v_1(p_T)$, the squeeze-out, $v_2(p_T)$, and the antiflow [27, 28, 29, 30, 31] (third flow component [32, 33]) serve as differential barometers for the properties of compressed, dense matter from SIS to RHIC. The most employed flow observables are:

$$v_1 = \left\langle \frac{p_x}{p_T} \right\rangle \tag{1}$$

$$v_2 = \left\langle \frac{p_x^2 - p_y^2}{p_x^2 + p_y^2} \right\rangle . \tag{2}$$

Here, p_x denotes the momentum in x-direction, i.e. the transversal momentum within the reaction plane and p_y the transversal momentum out of the reaction plane. The total transverse momentum is given as $p_T = \sqrt{p_x^2 + p_y^2}$; the z-axis is in the beam direction. Thus, flow v_1 measures the "bounce-off", i.e. the strength of the directed flow in the reaction plane, and v_2 gives the strength of the second moment of the azimuthal particle emission distribution, the so-called "squeeze-out". [24, 25, 27, 28, 29, 30, 31]. In particular, it has been shown [25, 27, 28, 29, 30, 31] that the disappearence or "collapse" of flow is a direct result of a first order phase transition.

Several hydrodynamic models have been used in the past, starting with the one-fluid ideal hydrodynamic approach. It is well known that the latter model predicts far too large flow effects. To obtain a better description of the dynamics, viscous fluid models have been developed [34, 35, 36]. In parallel, so-called three-fluid models, which distinguish between projectile, target and the fireball fluids, have been considered [37]. Here viscosity effects appear only between the different fluids, but not inside the individual fluids. The aim is to have at our disposal a reliable, three-dimensional, relativistic three-fluid model including viscosity [35, 36].

Flow can be described very elegantly in hydrodynamics. However, also consider microscopic multicomponent (pre-) hadron transport theory, e.g. models like qMD [38], IQMD [39], UrQMD [40] or HSD [41], as control models for viscous hydro and as background models to subtract interesting non-hadronic effects from data. If Hydro with and without quark matter EoS, hadronic transport models without quark matter – but with strings – are compared to data, can we learn whether quark matter has been formed? What degree of equilibration has been reached? What does the equation of state look like? How are the particle properties, self energies, cross sections changed?

To estimate systematic model uncertainties, the results of the different microscopic transport models also have to be carefully compared. The two robust hadron/string based models, HSD and UrQMD, are considered in the following.

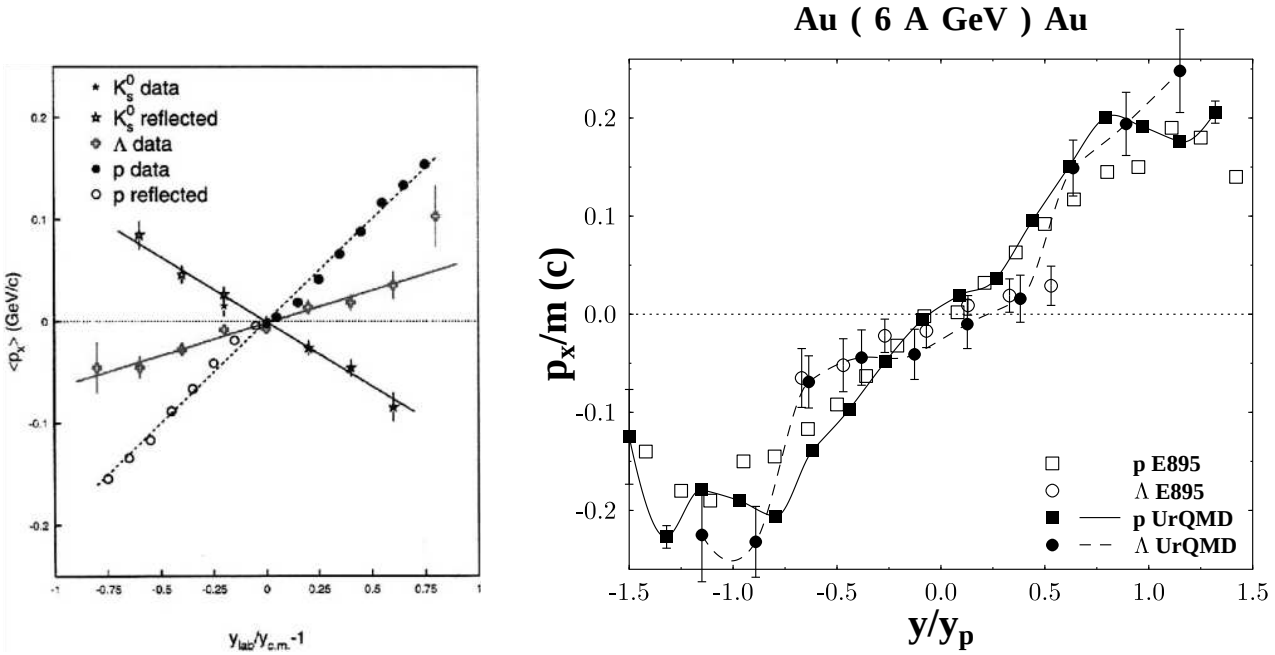

FIG. 4: Left: Sideward flow $p_x = v_1 \cdot p_T$ of K, Λ and p's at 6 A·GeV as measured by E895 in semi-central collisions at the AGS. Right: The same directed flow data for p and Λ compared to UrQMD calculations for $b < 7$ fm [45] .

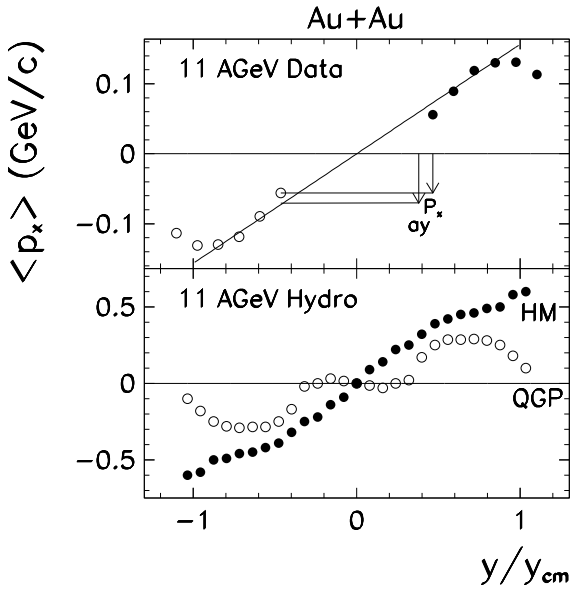

FIG. 5: Directed flow from ideal hydrodynamics with a QGP phase (open symbols) and from the Quark Gluon String Model without QGP phase (full symbols) [32] .

D. Review of AGS and SPS results

Microscopic (pre-)hadronic transport models describe the formation and distributions of many hadronic particles at AGS and SPS rather well [42]. Furthermore, the nuclear equation of state has been extracted by comparing to flow data which are described reasonably well up to AGS energies [32, 43, 44, 45, 46, 47]. Ideal hydro calculations, on the other hand, predict far too much flow at these energies [34]. Thus, viscosity effects have to be taken into account in hydrodynamics.

In particular, ideal hydro calculations are factors of two higher than the measured sideward flow at SIS [34] and AGS, while the directed flow p_x/m measurement of the E895 collaboration shows that the p and Λ data are reproduced reasonably well [45] (Fig. 4) in UrQMD, i.e. in a hadronic transport theory with reasonable cross-sections, i.e. realistic mean-free-path of the constituents.

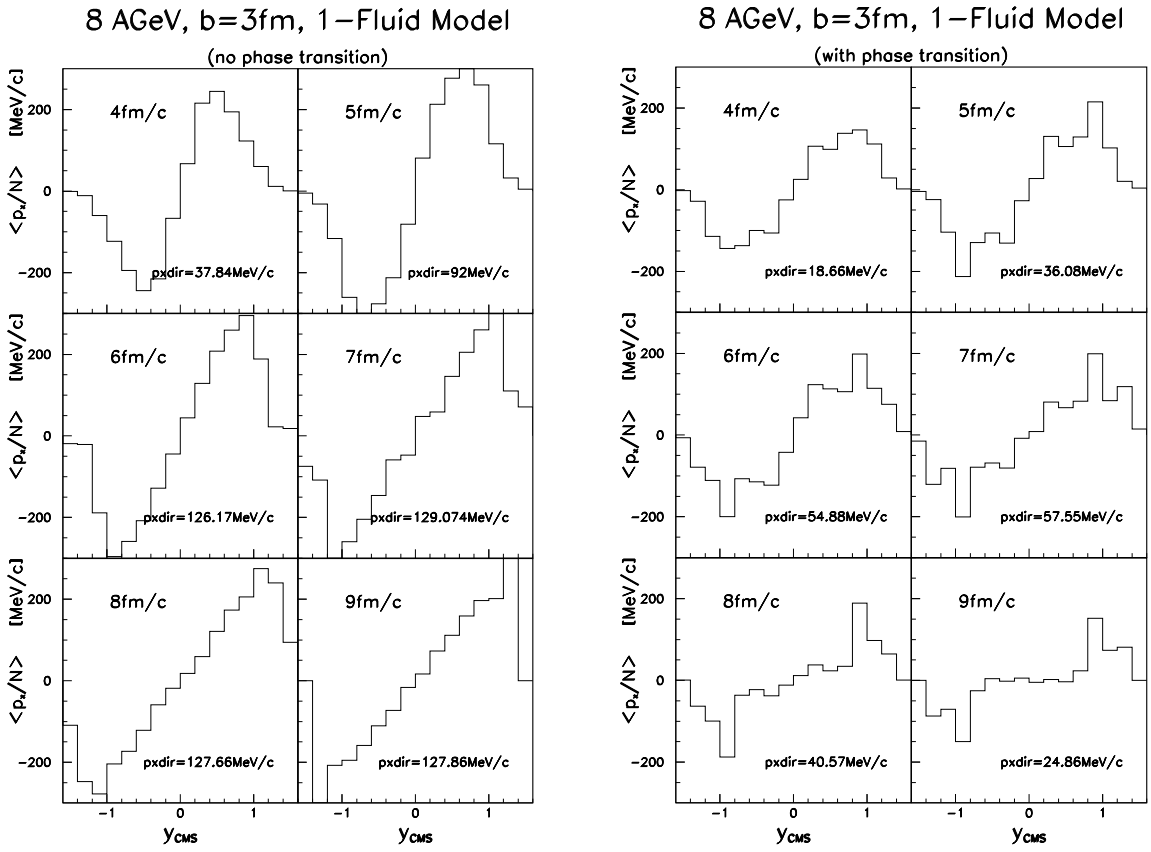

FIG. 6: Time evolution of directed flow p_x/N as a function of rapidity for Au+Au collisions at 8 A·GeV in the one-fluid model. Left: Hadronic EoS without phase transition. Right: An EoS including a first order phase transition to the QGP [48].

Only ideal hydro calculations predict, however, the appearance of a so-called "third flow component" [32] or "antiflow" [48] in central collisions (cf. Fig. 5). We stress that this only holds if the matter undergoes a first order phase transition to the QGP. The signal is that around midrapidity the directed flow, $p_x(y)$, of protons develops a negative slope! In contrast, a hadronic EoS without QGP phase transition does not yield such an exotic "antiflow" (negative slope) wiggle in the proton flow $v_1(y)$. The ideal hydrodynamic time evolution of the directed flow, p_x/N, for the purely hadronic EoS (Fig. 6 l.h.s.) does show a clean linear increase of $p_x(y)$, just as the microscopic transport theory (Fig. 4 r.h.s.) and as the data (Fig. 4 l.h.s.). For an EoS including a first order phase transition to the QGP (Fig. 6 r.h.s.) it can be seen, however, that the proton flow $v_1 \sim p_x/p_T$ collapses; the collapse occurs around midrapidity.

This observation is explained by an antiflow component of protons, which develops when the expansion from the plasma sets in [49].

The ideal hydrodynamic directed proton flow p_x (Fig. 7) shows even negative values between 8 and 20 A·GeV. An increase back to positive flow is predicted with increasing energy, when the compressed QGP phase is probed. But, where is the predicted minimum of the proton flow in the data? The hydro calculations suggest this "softest point collapse" is at $E_{Lab} \approx 8$ A·GeV. This has not been verified by the AGS data! However, a linear extrapolation of the AGS data indicates a collapse of the directed proton flow at $E_{Lab} \approx 30$ A·GeV (Fig. 7).

Recently, substantial support for this prediction has been obtained by the low energy 40 A·GeV SPS data of the NA49 collaboration [51] (cf. Fig. 8). These data clearly show the first proton "antiflow" around mid-rapidity, in contrast to the AGS data as well as to the UrQMD calculations involving no phase transition (Fig. 9). Thus, at bombarding energies of 30-40 A·GeV, a first order phase transition to the baryon rich QGP most likely is observed; the first order phase transition line is crossed (cf. Fig. 1). This is the energy region where the new FAIR- facility at GSI will operate. There are good prospects that the baryon flow collapses and other first order QGP phase transition signals can be studied soon at the lowest SPS energies as well as at the RHIC fragmentation region $y > 4 - 5$. These experiments will enable a detailed study of the first order phase transition at high μ_B and of the properties of the baryon rich QGP.

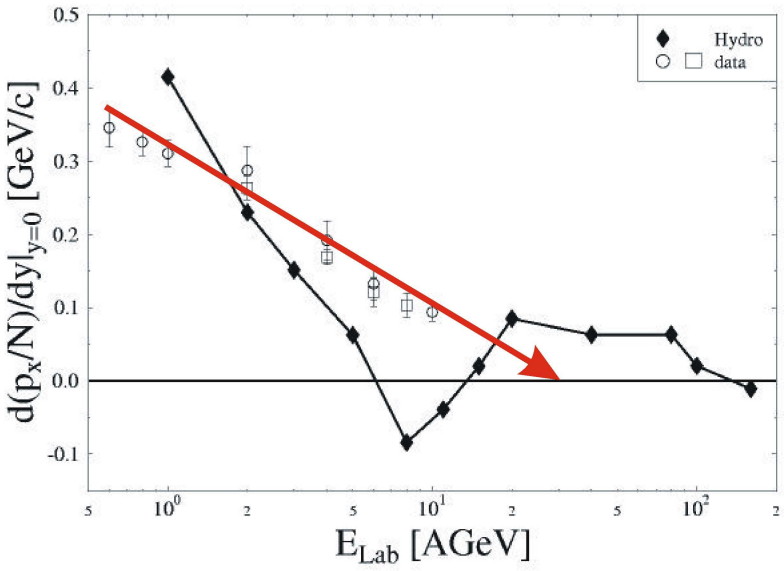

FIG. 7: Measured SIS and AGS proton dp_x/dy-slope data compared to a one-fluid hydro calculation. A linear extrapolation of the AGS data indicates a collapse of flow at $E_{Lab} \approx 30$ A·GeV, i.e. for the lowest SPS- and the upper FAIR- energies at GSI [50].

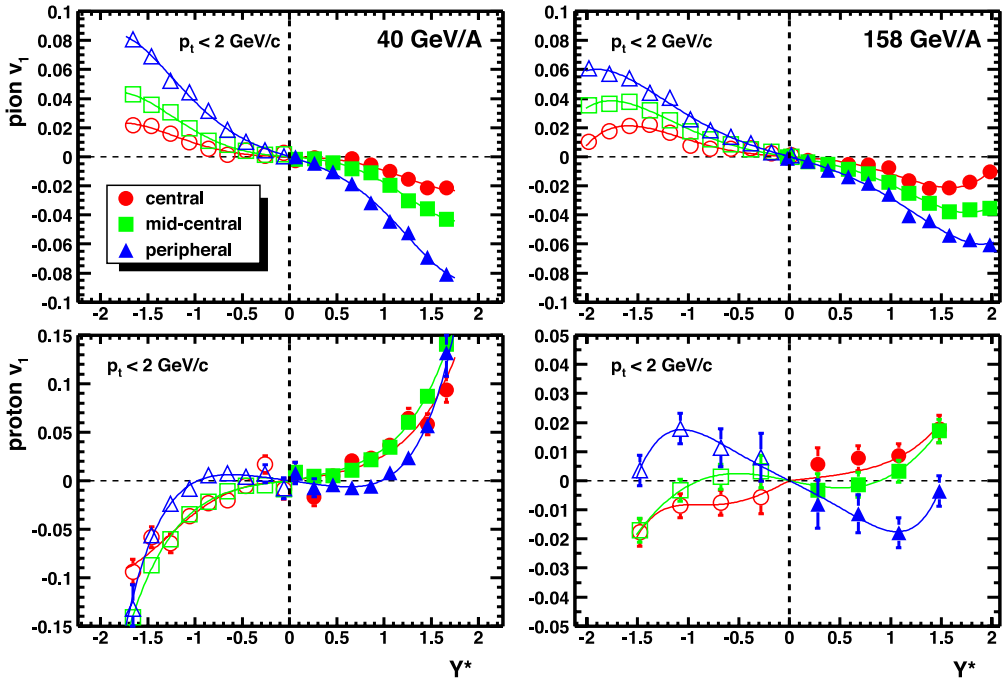

FIG. 8: v_1 at SPS, 40 A·GeV and 158 A·GeV [51] . The proton antiflow is observed in the NA49-experiment even at near central collisions, which is in contrast to the UrQMD-model involving no phase transition (Fig. 9).

II. PROTON ELLIPTIC FLOW COLLAPSE AT 40 A·GEV - EVIDENCE FOR A FIRST ORDER PHASE TRANSITION AT HIGHEST NET BARYON DENSITIES

At SIS energies microscopic transport models reproduce the data on the excitation function of the proton elliptic flow v_2 quite well: A soft, momentum-dependent equation of state [52, 53, 54] seems to account for the data. The observed proton flow v_2 below $\sim$ 5 A·GeV is smaller than zero, which corresponds to the squeeze-out predicted by

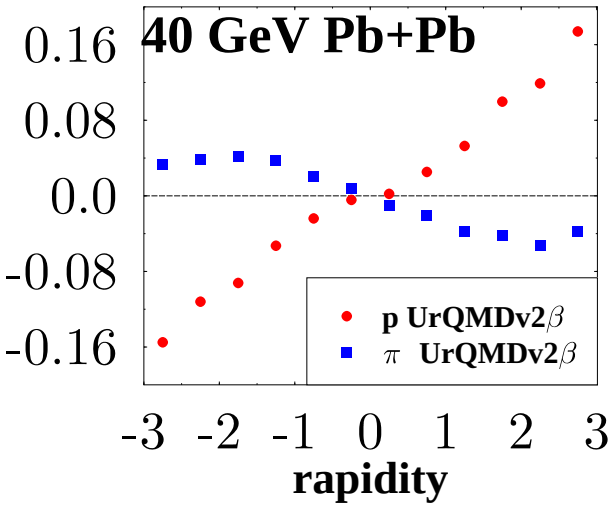

FIG. 9: Proton and pion flow $v_1 = p_x/p_T$ at 40 A·GeV as obtained within the UrQMD model. No proton antiflow is generated in this hadronic transport theory without phase transition.

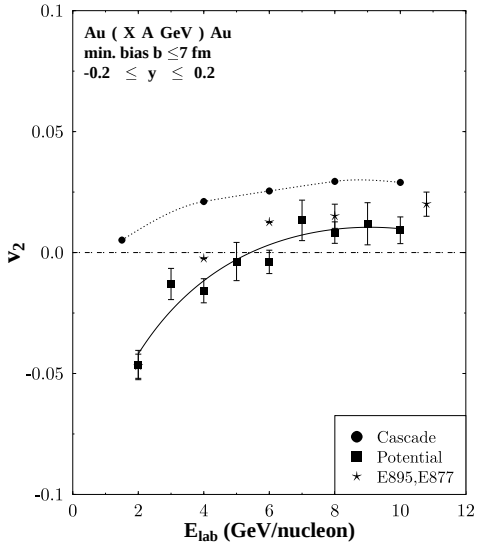

FIG. 10: v_2 excitation function of protons at the AGS. The E895-E877 data show the transition from squeeze-out to in-plane proton elliptic flow at 4-5 A·GeV; the UrQMD calculations show a strong sensitivity to the EoS [45].

hydrodynamics long ago [24, 25, 27, 28, 29, 30, 31]. The AGS data (Fig. 10) exhibit a transition from squeeze-out to in-plane flow in the midrapidity region. The change in sign of the proton v_2 at 4-5 A·GeV is in accord with transport calculations (UrQMD calculations in Fig. 10 [45]; for HSD results see [46, 47]). At higher energies, 10-160 A·GeV, a smooth increase of the flow v_2 is predicted from the hadronic transport simulations. In fact, the 158 A·GeV data of the NA49-collaboration suggest that this smooth increase proceeds between AGS and SPS as predicted. Accordingly, UrQMD gives considerable (3%) v_2 flow for midcentral and peripheral protons at 40 A·GeV – Fig. 11 [45].

This is in strong contrast to recent NA49 data at 40 A·GeV (cf. Fig. 12): A sudden collapse of the proton flow is observed for midcentral as well as for peripheral protons. This collapse of v_2 for protons around midrapidity at 40 A·GeV is very pronounced while it is not observed at 158 A·GeV. The UrQMD calculations, without a phase transition, show a robust, but wrong 3% flow of protons - in strong contrast to the data.

A dramatic collapse of the flow v_1 is also observed by NA49 [51], again around 40 A·GeV, where the collapse of v_2 has been observed. This is the highest energy - according to [1, 2] and Fig. 1 - at which a first order phase transition can be reached at the central rapidities of relativistic heavy-ion collisions. We, therefore, conclude that a first order phase transition at the highest baryon densities accessible in nature has been seen at these energies in

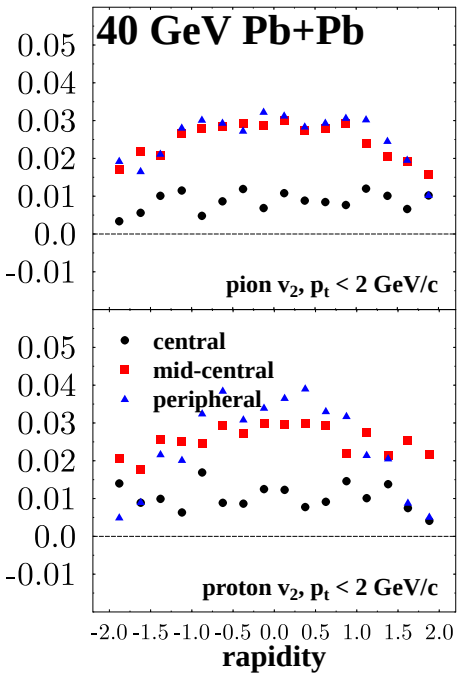

FIG. 11: Elliptic flow v_2 of protons (lower frame) and pions (upper frame) versus rapidity for Pb+Pb collisions at 40 A·GeV from the UrQMD calculations [45].

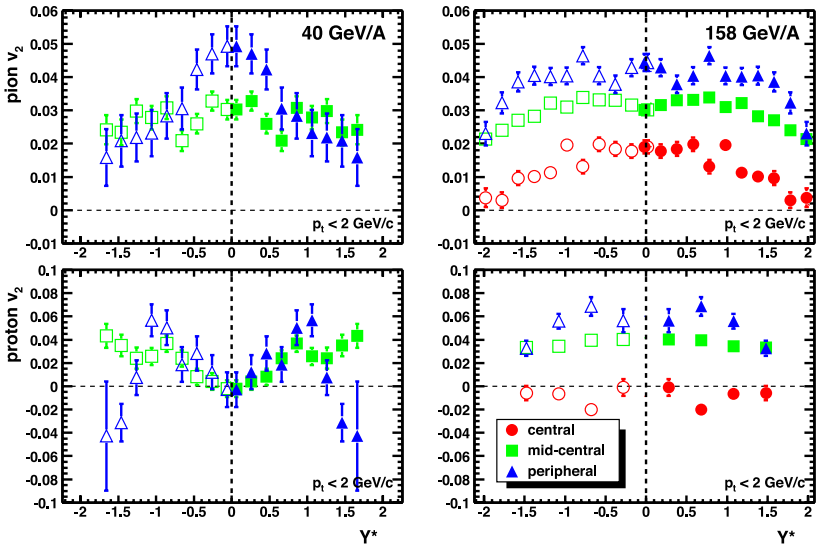

FIG. 12: Elliptic flow v_2 of protons versus rapidity at 40 A·GeV Pb+Pb collisions [51] as measured by NA49 for three centrality bins: central (dots), mid-central (squares) and peripheral (triangles). The solid lines are polynomial fits to the data [51].

Pb+Pb collisions. Moreover, Fig. 13 shows that the elliptic flow clearly distinguishes between a first order phase transition and a crossover.

III. STRONG COLLECTIVE FLOW AT RHIC SIGNALS A NEW PHASE OF MATTER

The rapid three-body thermalization found by Xu and Greiner (cf. Sec. IV.A) justifies *a posteriori* the use of hydrodynamical calculations for the time evolution of the complex four-dimensional expansion of the plasma. However, there is no justification for the use of simple ideal hydrodynamics (i.e. neglecting the important transport coefficients) and simple, smooth initial conditions in hydrodynamics [35, 36, 56]. PHOBOS data at $\sqrt{s_{NN}}$ = 130 GeV

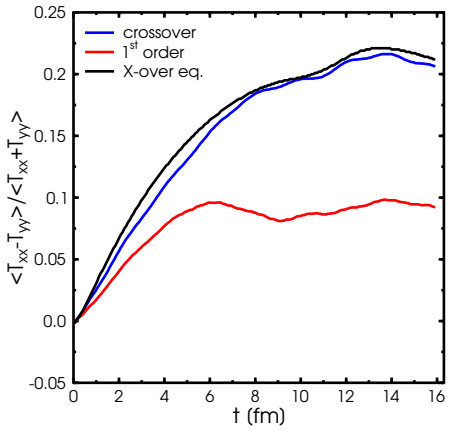

FIG. 13: Time evolution of the momentum anisotropy v_2 for a cross over EoS. Both, in- and off-equilibrium calculations (upper lines) show no drop of the flow v_2. The calculation with a first order phase transition off-equilibrium (lower line) shows - on the other hand - the collapse of v_2-flow of protons. Hence, the collapse is only possible for a first order transition [55].

and 200 GeV suggest energy independent $v_2(\eta)$ distributions. Furthermore, the observed distribution has a triangular shape. This finding is in strong disagreement with Bjorken boost invariant hydro predictions [12, 57], which fit only the midrapidity region. The predicted average proton v_2-values obtained from the SPHERIO hydro code with NEXUS initial conditons (Fig. 14, [58]) are by factors of two higher than simple smooth initial state hydrodynamic calculations. This indicates that ideal hydro with naive smooth initial conditions – as used by many authors – do not describe but rather fit the data. Strong viscosity effects can play a role for particles with $p_T < 1.2$ GeV/c: a decent description of the dynamics requires, however, relativistic viscous hydro simulations [35, 36, 59]. The NexSpherio simulations (Fig. 14, [58]) predict very large event-by-event fluctuations of v_2 caused by the strongly fluctuating initial conditions (given by NEXUS). Is this in accord with data? What about the effect on the event plane determination?

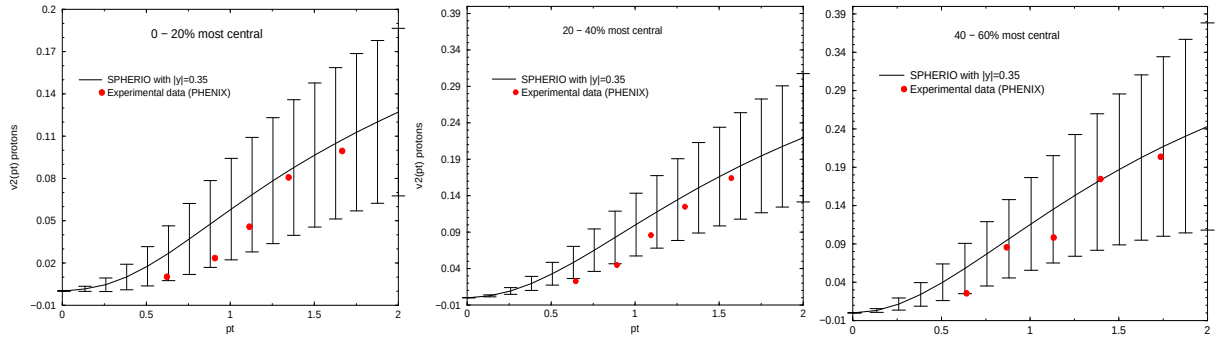

FIG. 14: Elliptic flow v_2 of protons as a function of p_T for different centralities. NexSpherio ideal hydro results exhibit about a factor of two higher proton-v_2-values than the PHENIX data up to $p_T = 1$ GeV/c. Furthermore, the fluctuations in the NEXUS initial conditions for the SPHERIO- ideal hydro simulation reflect > 50 % event-by-event fluctuations of the proton-v_2 values. Only large viscosity effects can damp out the too large v_2 flow itself as well as the fluctuations in v_2.

Microscopic transport simulations of particle yields, dN/dy distributions, etc. give a good description of the RHIC Au+Au data [19]. The HSD and UrQMD transport approaches are based on string, quark, diquark $(q, \bar{q}, qq, \bar{q}\bar{q})$ as well as hadronic degrees of freedom. At RHIC, UrQMD and HSD yield reasonable abundances of light hadrons composed of u, d, s quarks [1]. Do they also predict the collective flow properly? The UrQMD prediction is clearly not compatible with the measured 6% elliptic flow - it is sizeably underestimated [60]. When shortening the formation time [60] one can get the model results closer to the data (Fig. 15) but more additional initial pressure – needed to create the missing extra flow – is not justified in the hadronic transport models. At high transverse momenta ($p_T \approx 2$

[1] For a more recent survey on hadron rapidity distributions from 2 to 160 A·GeV in central nucleus-nucleus collisions within the HSD and UrQMD transport approaches we refer the reader to Ref. [42].

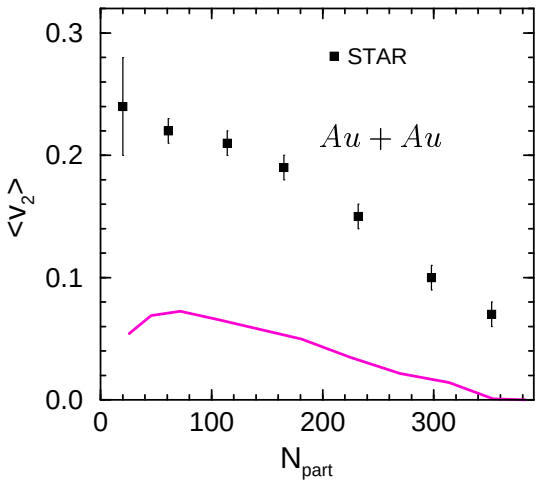

FIG. 15: High p_T- v_2 values as a function of N_{part} as measured by STAR are compared to HSD calculations. The v_2 data are more than 5 times higher than the HSD model predictions for the most central collisions [61].

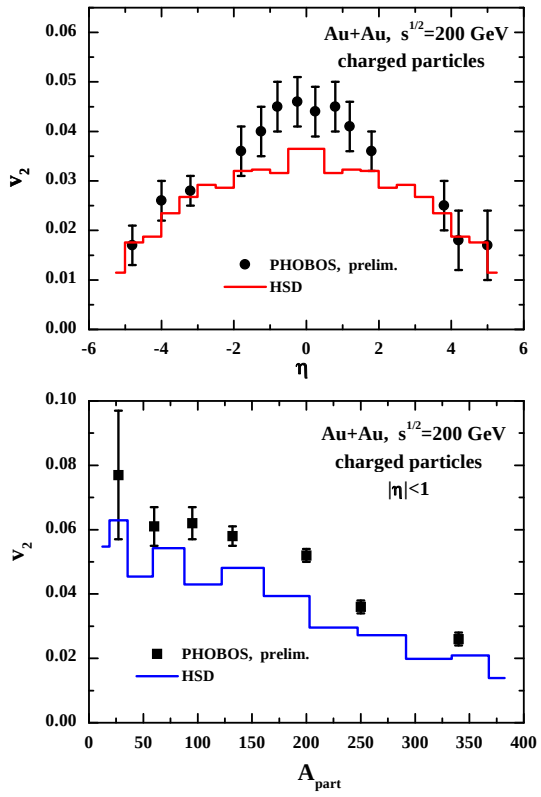

FIG. 16: The elliptic flow v_2 for charged hadrons (HSD, solid lines) as a function of pseudorapidity η (upper part) and as a function of the number of 'participating nucleons' A_{part} for $|\eta| \leq 1$ (lower part) for $Au + Au$ collisions at $\sqrt{s} = 200$ GeV, in comparison to the preliminary 'hit-based analysis' data of the PHOBOS Collaboration [63]. Note, that in spite of the shortened formation, $\tau \approx 0.8$ fm/c, HSD clearly underpredicts the data even at the moderate p_T-values dominating the p_T integrated v_2-values shown here. At higher p_T-values, Fig. 15, the discrepancy to the data is more dramatic.

GeV/c) the v_2-flow is underestimated even by a factor of three (Fig. 15) in the HSD model [61]. We mention that the microscopic quark-gluon-string model inserts in addition short distance vector repulsion in order to achieve high flow values [62].

Is a transport approach – based on strings and hadronic degrees of freedom – adequate in the initial stage of nucleus-nucleus collisions at RHIC energies, where the quark-gluon plasma is formed? Well, the particle abundancies

show a rather smooth evolution from SIS to RHIC energies [64, 65]. However, the effective partonic degrees of freedom in the initial phase are needed to supply the large pressure obviously needed to describe the elliptic flow at RHIC energies. Even 'early' hadron formation – as in HSD with $\tau = 0.8$ fm/c – and 'large' (pre-)hadronic interaction cross sections are insufficient to explain the v_2 flow data. This is demonstrated in Fig. 16, which shows the calculated elliptic flow v_2 from HSD for charged hadrons (solid lines) as a function of the pseudorapidity η (upper part) and as a function of the number of 'participating nucleons' N_{part} (lower part) for $|\eta| \leq 1$ in comparison to the preliminary 'hit-based analysis' data of the PHOBOS Collaboration [63]. The HSD results are very similar to those of the hadronic rescattering model by Humanic et al. [66, 67] and agree with the calculations by Sahu et al. [68] performed within the hadron-string cascade model JAM [69].

IV. EARLY THERMALIZATION AT RHIC - EVIDENCE FOR A NEW PHASE

A. Elastic and inelastic multi-particle collisions in a parton cascade

To describe the early dynamics of ultrarelativistic heavy-ion collisions and to address the crucial question of thermalization and the early pressure build up at RHIC, unexpectedly high elastic parton cross sections have been assumed in parton cascades [70, 71] in order to reproduce the elliptic flow $v_2(p_T)$ seen experimentally at RHIC. These cross sections are about 1/9 of the baryon-baryon total cross section ($\sim$ 45 mb) or 1/6 of the meson-baryon cross section ($\sim$ 30 mb), such that the effective cross section for the constituent quarks and antiquarks is roughly the same in the partonic and hadronic phase, however, tenfold higher than the cross sections calculated in pQCD.

It has been a great puzzle until recently, when Xu and Greiner developed a consistent three-body kinetic parton cascade algorithm [72, 73]. These stochastic inelastic ('Bremsstrahlung') $2 \rightarrow 3$ and $3 \rightarrow 2$ collisions ($gg \leftrightarrow ggg$) drive early thermalization, rather than the two-body elastic collisions, which are too strongly forward peaked. A quantitative understanding of the early dynamical stages of deconfined matter is finally in sight. Parton cascade analyses incorporating only binary $2 \leftrightarrow 2$ pQCD scattering processes can not build up thermalization and early quasi-hydrodynamic behaviour necessary for achieving sufficient elliptic flow. The importance of inelastic reactions was raised in the so called 'bottom-up thermalization' picture [74]; gluon multiplication leads to a much faster equilibration.

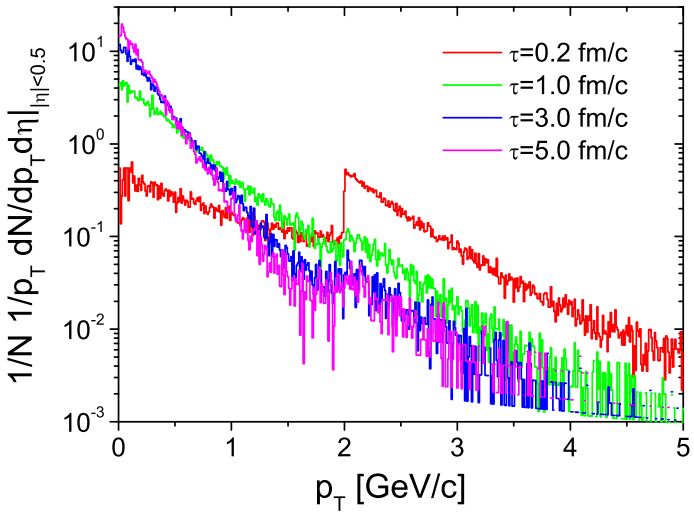

FIG. 17: Time evolution of the midrapidity transverse momentum spectrum for a central RHIC collision from the three-dimensional Xu-Greiner-parton cascade simulation [72, 73] (prelimenary results are from [75] - including transverse expansion). Only partons residing in a central cylinder of radius $R \leq 5$ fm are plotted. The initial off-equilibrium conditions are given by a minijet distribution with corresponding overlap function in space-time. At $t = 0$, only minijets with $p_T > 2$ GeV/c are populated. Energy degradation to lower momenta proceeds by rapid gluon emission within the first fm/c. (Quasi-)kinetic and chemical equilibrium is found up to 4 fm/c. Here longitudinal and transversal hydrodynamic work is at action, resulting in a rapid lowering of the temperature by a factor of two. On the other hand, a small fraction of the initial non-equilibrium high momentum power-law tail of the mini-jet production survives even in this central cell.

Xu and Greiner consider - besides gluon- and quark- two-body elementary parton-parton scatterings - three-body processes $gg \leftrightarrow ggg$ in leading-order pQCD. They employ effective Landau-Pomeranchuk-Migdal suppression and standard screening masses for the infrared sector of the scattering amplitude.

The early stage of gluon production in the Xu-Greiner (X-G) approach (Fig. 17) leads to a rapid kinetic equilibration of the momentum distribution as well as to a rather abrupt lowering of the temperature by soft gluon emission. Detailed balance among gain and loss contributions is reached rapidly, too. The later, slower time evolution is then governed by chemical equilibration of the quark degrees of freedom. The X-G cascade does allow to study in detail RHIC-collisions with various initial conditions like minijets or color glass condensate (CGC). Fig. 17 depicts a preliminary calculation [75] using minijet-initial conditions.

Thermalization and chemical equilibration – as proposed in the bottom-up scenario [74] – can thoroughly be tested within this approach. The impact parameter dependence on the transverse energy is used to understand elliptic and transverse flow at RHIC within this new kinetic parton cascade with inelastic $3 \rightarrow 2$ and $2 \rightarrow 3$ interactions.

V. HOW MUCH QUENCHING OF HIGH p_T HADRONS IS DUE TO (PRE-) HADRONIC FINAL STATE INTERACTIONS?

A (mini-)jet at RHIC can produce hard particles, with p_T above 5 GeV/c, but must also form soft particles with p_T around 2 GeV/c. Jets produced in the center of the plasma zone have to pass first through the parton phase at very high temperatures, then through the correlated diquark and constituent quarks and finally through the hadronic phase that has build up preferentially close to the surface of the fireball. Very high p_T jets with $\gamma > 10$ materialize only far outside of the plasma. Most of the jets – observed at RHIC – are at $p_T \approx 4 - 5$ GeV/c. More than 50% of the leading jet particles at $p_T \sim 5\,\mathrm{GeV/c}$ are baryons. Pion jets of 5 GeV have a $\gamma = 35$, i.e., they form far outside the plasma. However, HSD-PYTHIA-calculations [76] show that many pions stem from decaying rho-jets. But, ρ's and protons of 5 GeV have $\gamma = 5$. Thus, ρ and p-jets hadronize with roughly 50% probability [61, 77] while passing through the expanding bulk matter. All partonic and hadronic models have failed by factors of 5-10 to predict the observed high baryon abundance.

The PHENIX [78] and STAR [79] collaborations reported a suppression of meson spectra for transverse momenta p_T above $\sim 3\,\mathrm{GeV/c}$. This suppression is not observed in d+Au interactions at the same bombarding energy per nucleon [80, 81] and presents clear evidence for the presence of a new form of matter. However, it is not clear at present how much of the observed suppression can be attributed to (pre-)hadronic interactions (FSI) [77]. (In-)elastic collisions of (pre-)hadronic high momentum states with some of the bulk (pre-)hadrons in the fireball can contribute in particular to the attenuation of $p_T \approx 5\,\mathrm{GeV/c}$ transverse momentum hadrons at RHIC [76]: Most of the medium momentum (pre-)hadrons from a ± 5 GeV/c double jet will materialize inside the dense plasma; their transverse momenta being 0-4 GeV/c. The particles are dominantly ρ's, K's and baryons at $p_T > 2.5\,\mathrm{GeV/c}$ – hence their formation time is $\gamma\tau_F \approx 4$ fm/c in the plasma rest frame. The time for color neutralization can also be very small [82] for the leading particle due to early gluon emission.

The (pre-)hadronic interactions with the bulk of the (pre-)hadronic comovers then must have clearly an effect: they, too, suppress the p_T-spectrum [77]. (In)elastic reactions of the fragmented (pre-)hadrons with (pre-)hadrons of the bulk system cannot be described by pQCD: The relevant energy scale $\sqrt{s}$ is a few GeV. Such (in-)elastic collisions are very efficient for energy degradation since many hadrons with lower energies are produced. On the average, 1 to 2 such interactions can account for up to 50% of the attenuation of high p_T hadrons at RHIC [77]. Hence, the hadronic fraction of the jet-attenuation had to be addressed.

In Ref. [61] the HSD transport approach [41] is employed. Moderate to high transverse momenta (> 1.5 GeV/c) are incorporated by a superposition of $p+p$ collisions described via PYTHIA [14]. In Au+Au collisions, the formation of secondary hadrons is not only controlled by the formation time τ_f, but also by the energy density in the local rest frame. In [61], hadrons are not allowed to be formed if the energy density is above 1 GeV/fm^3[2]. The interaction of the leading and energetic (pre-)hadrons with the soft hadronic and bulk matter is thus explicitly modeled.

Figs. 18, 19 show the nuclear modification factor [76]

$$R_{\mathrm{AA}}(p_T) = \frac{1/N_{\mathrm{AA}}^{\mathrm{event}}\; d^2N_{\mathrm{AA}}/dydp_T}{\langle N_{\mathrm{coll}}\rangle /\sigma_{pp}^{\mathrm{inelas}}\; d^2\sigma_{pp}/dydp_T}\ . \tag{3}$$

for the most central (5% centrality) Au+Au collisions at RHIC. The Cronin enhancement is visible at all momenta. Hadron formation time effects do play a substantial role in the few GeV region, since heavier hadrons (K*'s, ρ's,

[2] This energy density criterion is employed in the default HSD approach.

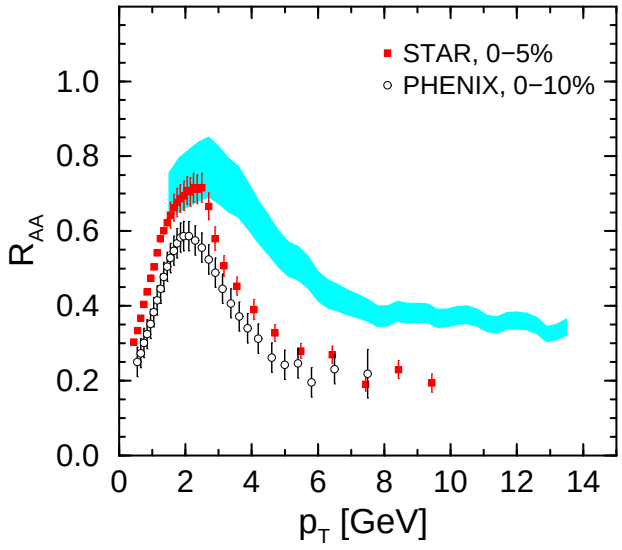

FIG. 18: The suppression factor R_{AA} (3) of charged hadrons at 5% (10%) central $Au + Au$ collisions ($\sqrt{s}$=200 GeV) at midrapidity (hatched band). The experimental data are from Refs. [23, 85] and show clearly that an additional partonic suppression is needed (taken from Ref. [61]).

protons) are formed 7 times earlier than the rather light pions in the cms frame at fixed transverse momentum due to the lower Lorentz boost $\gamma < 5$. It was shown in [61] that for transverse momenta $p_T \geq 6$ GeV/c the interactions of formed hadrons are not able to explain the attenuation observed experimentally. However, the ratio $R_{\rm AA}$ is influenced by interactions of formed (pre-)hadrons in the $p_T = 1 \ldots 5\,{\rm GeV}/c$ range [61]. A similar behaviour has also been found in UrQMD simulations [83].

As pointed out before, the suppression seen in the calculation for larger transverse momentum hadrons is due to the interactions of the leading (pre-)hadrons with target/projectile nucleons and the bulk of low momentum hadrons. It is clear that the experimentally observed suppression can not be quantitatively described by the (pre-)hadronic attenuation of the leading particles [61]. The ratio $R_{\rm AA}$ (3) decreases to a value of about 0.5 at 5 GeV for central collisions, whereas the data are around $R_{\rm AA} \approx 0.25$.

To check, how robust this HSD estimate is, alternative models for the leading pre-hadron cross section have been

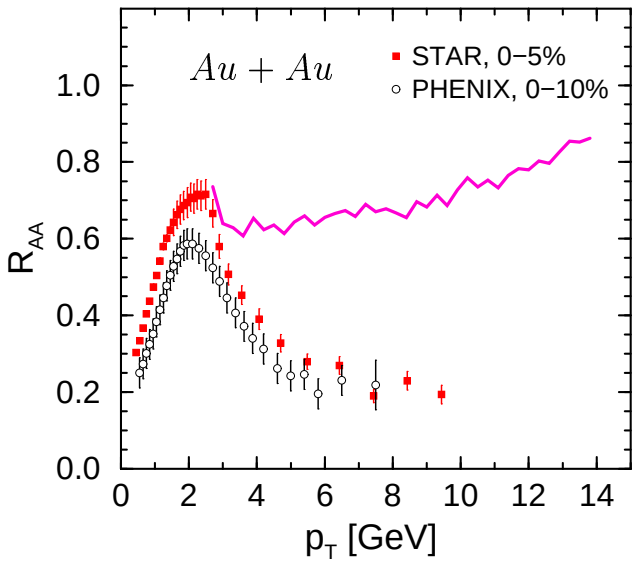

FIG. 19: Same as Fig. 18, but with a leading cross section according to eq. (4) for the perturbative high p_T particles. The observed attenuation is more than double the value!

studied in [61] by adopting a time–dependent, color-transparency-motivated cross section for leading pre-hadrons [84]

$$\sigma_{\rm lead}(\sqrt{s},\tau) = \frac{\tau-\tau_0}{\tau_f}\sigma_{\rm had}(\sqrt{s}) \tag{4}$$

for $\tau - \tau_0 \leq \tau_f$, where τ_0 denotes the actual production time, τ_f the formation time, after which the full hadronic cross section is reached.

Within this scenario the attenuation is 35% at $p_T \sim 5\,{\rm GeV}/c$ (see Fig. 19), while the data show more than double the attenuation. Thus, (pre-)hadronic jet interactions cannot provide a quantitative explanation for the jet suppression observed. They do provide, however, a sizable $(30-50\%)$ contribution to the jet quenching.

For particles observable with momenta $p_T \geq 4$ GeV/c, the HSD transport calculation predicts that still 1/3 of the final observed hadrons have suffered one or more interactions, whereas the other 2/3 escape freely, i.e., without any interaction (even for central collisions). This implies that the final high p_T hadrons originate basically from the surface.

A. Angular Correlations of Jets – Can jets fake the large v_2-values observed?

Fig. 20 [76] shows the angular correlation of high p_T particles ($p_T NTrig = 4\ldots6\,{\rm GeV}/c$, $p_T = 2\,{\rm GeV}\ldots p_T NTrig$, $|y| < 0.7$) for the 5% most central Au+Au collisions at $\sqrt{s} = 200$ GeV (solid line) as well as pp reactions (dashed line) from the HSD-model [76] in comparison to the data from STAR for pp collisions [86]. Gating on high p_T hadrons (in the vacuum) yields 'near–side' correlations in Au+Au collisions close to the 'near–side' correlations observed for jet fragmentation in the vacuum (pp). This is in agreement with the experimental observation [86]. However, for the away-side jet correlations, the authors of Ref. [76] get only a ∼50% reduction, similar to HIJING, which has only parton quenching and neglects hadron rescattering. Clearly, the observed [86] complete disappearance of the away-side jet (Fig. 20) cannot be explained in the HSD-(pre-)hadronic cascade even with a small formation time of 0.8 fm/c. Hence, the correlation data provide another clear proof for the existence of the bulk plasma.

Although (pre-)hadronic final state interactions yield a sizable ($\leq 50\%$) contribution to the high p_T suppression effects observed in Au+Au collisions at RHIC, $\sim 50\%$ of the jet suppression originates from interactions in the plasma phase. The elliptic flow, v_2, for high transverse momentum particles is underestimated by at least a factor of 3 in the HSD transport calculations [61] (cf. Fig. 15). The experimentally observed proton excess over pions at transverse momenta $p_T > 2.5$ GeV/c cannot be explained within the CGG approach [61]; in fact, the proton yield at high $p_T \geq 5$ GeV/c is a factor 5-10 too small. We point out that this also holds for partonic jet-quenching models. Further experimental data on the suppression of high momentum hadrons from d+Au and Au+Au collisions, down to $\sqrt{s} =$ 20 GeV, are desperately needed to separate initial state Cronin effects from final state attenuation and to disentangle the role of partons in the colored parton plasma from those of interacting pre-hadrons in the hot and dense fireball.

Can the attenuation of jets of $p_T \geq 5\,{\rm GeV}/c$ actually fake the observed v_2-values at $p_T \approx 2\,{\rm GeV}/c$? This question comes about since due to fragmentation and rescattering a lot of momentum-degraded hadrons will propagate in the hemisphere defined by the jets. However, their momentum dispersion perpendicular to the jet direction is so large that it could indeed fake a collective flow that is interpreted as coming from the high pressure early plasma phase.

On first sight, Fig. 21 shows that this could indeed be the case: the in-plane v_2 correlations are aligned with the jet axis, the away-side bump, usually attributed to collective v_2 flow (dashed line), could well be rather due to the stopped, fragmented and rescattered away-side jet! However, this argument is falsified by the out-of-plane correlations (circles in Fig. 21). The near-side jet is clearly visible in the valley of the collective flow v_2 distribution. Note that v_2 peaks at $\varphi = \pi/2$ relative to the jet axis! The away-side jet, on the other hand, has completely vanished in the out-of-plane distribution (cf. Fig. 22)!

Where are all the jet fragments gone? Why is there no trace left? Even if the away-side jet fragments completely and the fragments get stuck in the plasma, leftovers should be detected at momenta below $2\,{\rm GeV}/c$. Hadronic models as well as parton cascades will have a hard time to get a quantitative agreement with these exciting data!

We propose future correlation measurements which can yield spectroscopic information on the plasma.

1. If the plasma is a colorelectric plasma, experiments will - in spite of strong plasma damping - be able to search for wake-riding potential effects. The wake of the leading jet particle can trap comoving companions that move through the plasma in the wake pocket with the same speed (p_T/m) as the leading particle. This can be particular stable for charmed jets due to the deadcone effect as proposed by Kharzeev et al [87], which will guarantee little energy loss, i.e. constant velocity of the leading D-meson. The leading D-meson will practically have very little momentum degradation in the plasma and therefore the wake potential following the D will be able to capture the equal speed companion, which can be detected [88].

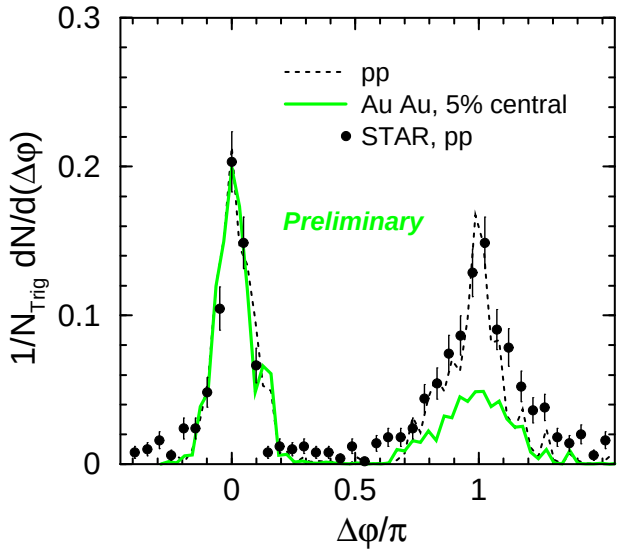

FIG. 20: STAR data on near-side and away-side jet correlations compared to the HSD model for p+p and central Au+Au collisions at midrapidity for $p_T NTrig = 4 \ldots 6\,\mathrm{GeV}/c$ and $p_T = 2\,\mathrm{GeV}/c \ldots p_T NTrig$. [61, 76]

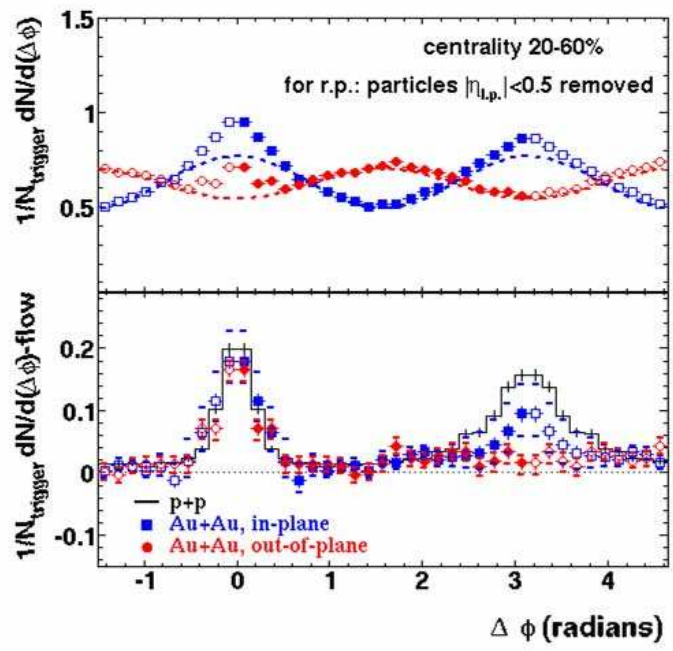

FIG. 21: High p_T correlations: in-plane vs. out-of-plane correlations of the probe (jet+secondary jet fragments) with the bulk (v_2 of the plasma at $p_T > 2\,\mathrm{GeV/c}$), prove the existence of the initial plasma state (STAR-collaboration, preliminary).

2. One may measure the sound velocity of the expanding plasma by the emission pattern of the plasma particles travelling sideways with respect to the jet axis: The dispersive wave generated by the wake of the jet in the plasma yields preferential emission to an angle (relative to the jet axis) which is given by the ratio of the leading jet particles' velocity, devided by the sound velocity in the hot dense plasma rest frame. The speed of sound for a non-interacting gas of relativistic massless plasma particles is $c_s \approx \frac{1}{\sqrt{3}} \approx 57\%\, c$, while for a plasma with strong vector interactions, $c_s = c$. Hence, the emission angle measurement can yield information of the interactions in the plasma.

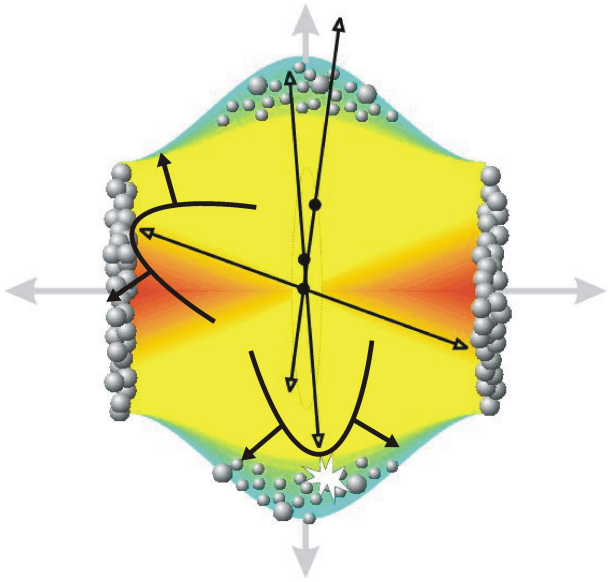

FIG. 22: Illustration of jets traveling through the late hadronic stage of the reaction. Only jets from the region close to the initial surface can propagate and fragment in the vacuum [24, 76, 89, 90]. The other jets will interact with the bulk, resulting in wakes with bow waves travelling transversely to the jet axis.

VI. SUMMARY

The NA49 collaboration has observed the collapse of both, v_1- and v_2-collective flow of protons, in Pb+Pb collisions at 40 A·GeV, which presents first evidence for a first order phase transition in baryon-rich dense matter. It will be possible to study the nature of this transition and the properties of the expected chirally restored and deconfined phase both at the forward fragmentation region at RHIC, with upgraded and/or second generation detectors, and at the new GSI facility FAIR. According to Lattice QCD results [1, 2], the first order phase transition occurs for chemical potentials above 400 GeV. Fig. 13 shows that the elliptic flow clearly distinguishes between a first order phase transition and a crossover. Thus, the observed collapse of flow, as predicted in [24, 25], is a clear signal for a first order phase transition at the highest baryon densities.

A critical discussion of the use of collective flow as a barometer for the equation of state (EoS) of hot dense matter at RHIC showed that hadronic rescattering models can explain $< 30\%$ of the observed flow, v_2, for $p_T > 2$ GeV/c. We interpret this as evidence for the production of superdense matter at RHIC with initial pressure way above hadronic pressure, $p > 1$ GeV/fm^3.

The fluctuations in the flow, v_1 and v_2, should be measured. Ideal Hydrodynamics predicts that they are larger than 50 % due to initial state fluctuations. The QGP coefficient of viscosity may be determined experimentally from the fluctuations observed.

The connection of v_2 to jet suppression is examined. It is proven experimentally that the collective flow is not faked by minijet fragmentation and that the away-side jet suppression can only partially ($< 50\%$) be due to pre-hadronic or hadronic rescattering.

We propose upgrades and second generation experiments at RHIC, which inspect the first order phase transition in the fragmentation region, i.e. at $\mu_B \approx$ 400 MeV ($y \approx 4 - 5$), where the collapse of the proton flow analogous to the 40 A·GeV data should be seen.

The study of Jet-Wake-riding potentials and Bow shocks caused by jets in the QGP formed at RHIC can give further clues on the equation of state and transport coefficients of the Quark Gluon Plasma.

Acknowledgments

I like to thank E. L. Bratkovskaya, M. Bleicher, A. Muronga, K. Paech, M. Reiter, S. Scherer, S. Soff, H. Weber, G. Zeeb, D. Zschiesche, W. Cassing, C. Greiner, K. Gallmeister, Z. Xu, B. Tavares, L. Portugal, C. Aguiar, T. Kodama,

F. Grassi, Y. Hama, T. Osada, O. Sokolowski, and K. Werner for their contributions that have made this review possible.

---

[1] Z. Fodor and S. D. Katz, JHEP **0203** (2002) 014; JHEP **0404** (2004) 050.
[2] F. Karsch, hep-lat/0403016.
[3] R. Anishetty, Peter Koehler, and Larry D. McLerran, Phys. Rev. **D 22** (1980) 2793.
[4] S. Date, M. Gyulassy, and H. Sumiyoshi, Phys. Rev. **D 32** (1985) 619.
[5] P. Koch, B. Müller, and J. Rafelski, Phys. Rept. **142** (1986) 167.
[6] C. Greiner, P. Koch, and H. Stöcker, Phys. Rev. Lett. **58** (1987) 1825.
[7] C. Greiner, D. Rischke, H. Stöcker, and P. Koch, Phys. Rev. **D 38** (1988) 2797.
[8] L. V. Bravina *et al.*, Phys. Rev. **C 60** (1999) 024904; Nucl. Phys. **A 698** (2002) 383.
[9] E. L. Bratkovskaya *et al.*, Phys. Rev. C, in press; nucl-th/0402026.
[10] J. Cleymans and K. Redlich, Phys. Rev. **C60** (1999) 054908.
[11] I. G. Bearden *et al.*, Phys. Rev. Lett. **90** (2003) 102301.
[12] E. Shuryak, Nucl. Phys. **A 661** (1999) 119.
[13] W. Cassing, K. Gallmeister, E. L. Bratkovskaya, C. Greiner, and H. Stöcker, Prog. Part. Nucl. Phys. **53** (2004) 211.
[14] T. Sjostrand *et al.*, Comput. Phys. Commun. **135** (2001) 238.
[15] W. Cassing, E. L. Bratkovskaya, and A. Sibirtsev, Nucl. Phys. **A 691** (2001) 753.
[16] W. Cassing, E. L. Bratkovskaya, and S. Juchem, Nucl. Phys. **A 674** (2000) 249.
[17] W. Cassing and E. L. Bratkovskaya, Nucl. Phys. **A 623** (1997) 570.
[18] C. Spieles *et al.*, J. Phys. **G 25** (1999) 2351.
[19] E. L. Bratkovskaya, W. Cassing, and H. Stöcker, Phys. Rev. **C 67** (2003) 054905.
[20] L. Ramello *et al.*, Nucl. Phys. **A 715** (2003) 243.
[21] H. Satz, Rept. Prog. Phys. **63** (2000) 1511.
[22] L. Grandchamp and R. Rapp, Phys. Lett. **B 523** (2001) 60.
[23] J. L. Nagle, Nucl. Phys. **A 715** (2003) 252.
[24] J. Hofmann, H. Stöcker, W. Scheid, and W. Greiner, Report of the workshop on BeV/nucleon collisions of heavy ions - how and why, Bear Mountain, New York, Nov. 29 - Dec. 1, 1974 (BNL-AUI 1975).
[25] J. Hofmann, H. Stöcker, U. W. Heinz, W. Scheid, and W. Greiner, Phys. Rev. Lett. **36** (1976) 88.
[26] L.D. Landau and E.M. Lifshitz, Fluid Mechanics, Pergamon Press, New York, 1959.
[27] H. Stöcker, J. Hofmann, J. A. Maruhn, and W. Greiner, Prog. Part. Nucl. Phys. **4** (1980) 133.
[28] H. Stöcker, J. A. Maruhn, and W. Greiner, Phys. Rev. Lett. **44** (1980) 725.
[29] H. Stöcker *et al.*, Phys. Rev. Lett. **47** (1981) 1807.
[30] H. Stöcker *et al.*, Phys. Rev. **C 25** (1982) 1873.
[31] H. Stöcker and W. Greiner. Phys. Rept. **137** (1986) 277.
[32] L. P. Csernai and D. Rohrich, Phys. Lett. **B 458** (1999) 454.
[33] L. P. Csernai *et al.*, hep-ph/0401005.
[34] W. Schmidt *et al.*, Phys. Rev. **C 47** (1993) 2782.
[35] A. Muronga, Heavy Ion Phys. **15** (2002) 337.
[36] A. Muronga, Phys. Rev. **C 69** (2004) 034903.
[37] J. Brachmann *et al.*, Nucl. Phys. **A 619** (1997) 391.
[38] M. Hofmann *et al.*, nucl-th/9908031.
[39] C. Hartnack *et al.*, Nucl. Phys. **A 495** (1989) 303c.
[40] S. A. Bass, M. Gyulassy, H. Stöcker, and W. Greiner, J. Phys. **G 25** (1999) R1.
[41] W. Cassing and E. L. Bratkovskaya, Phys. Rept. **308** (1999) 65.
[42] H. Weber, E. L. Bratkovskaya, W. Cassing, and H. Stöcker, Phys. Rev. **C 67** (2003) 014904.
[43] A. Andronic *et al.*, Phys. Rev. **C 67** (2003) 034907.
[44] A. Andronic *et al.*, Phys. Rev. **C 64** (2001) 041604.
[45] S. Soff, S. A. Bass, M. Bleicher, H. Stöcker, and W. Greiner, nucl-th/9903061.
[46] P. K. Sahu and W. Cassing, Nucl. Phys. **A 672** (2000) 376.
[47] P. K. Sahu and W. Cassing, Nucl. Phys. **A 712** (2002) 357.
[48] J. Brachmann, PhD thesis, J. W. Goethe Universität Frankfurt am Main, 2000.
[49] J. Brachmann *et al.*, Phys. Rev. **C 61** (2000) 024909.
[50] K. Paech, M. Reiter, A. Dumitru, H. Stöcker, and W. Greiner, Nucl. Phys. **A 681** (2001) 41.
[51] C. Alt *et al.*, Phys. Rev. **C 68** (2003) 034903.
[52] A. Andronic *et al.*, Nucl. Phys. **A 679** (2001) 765.
[53] A. Andronic, Nucl. Phys. **A 661** (1999) 333.
[54] A. Larionov *et al.*, Phys. Rev. **C 62** (2000) 064611.
[55] K. Paech, H. Stöcker, and A. Dumitru, Phys. Rev. **C 68** (2003) 044907.
[56] D. A. Teaney, nucl-th/0403053.

[57] U. Heinz and P. F. Kolb, nucl-th/0403044.
[58] C. E. Aguiar, Y. Hama, T. Kodama, and T. Osada, Nucl. Phys. **A 698** (2002) 639.
[59] A. Muronga, Phys. Rev. **C 69** (2004) 044901.
[60] M. Bleicher and H. Stöcker, Phys. Lett. **B 526** (2002) 309.
[61] W. Cassing, K. Gallmeister, and C. Greiner, Nucl. Phys. **A 735** (2004) 277.
[62] E. Zabrodin, L. Bravina, C. Fuchs, and A. Faessler, hep-ph/0403022.
[63] S. Manly *et al.*, Nucl. Phys. **A 715** (2003) 611.
[64] J. L. Nagle and T. S. Ullrich, nucl-ex/0203007.
[65] B. B. Back *et al.*, Nucl. Phys. **A 715** (2003) 65.
[66] T. J. Humanic, nucl-th/0203004.
[67] R. Bellwied, H. Caines, and T. J. Humanic, Phys. Rev. **C 62** (2000) 054906.
[68] P. K. Sahu, N. Otuka, and A. Ohnishi, nucl-th/0206010.
[69] Y. Nara, N. Otuka, A. Ohnishi, K. Niita, and S. Chiba, Phys. Rev. **C 61** (2000) 024901.
[70] B. Zhang, C. M. Ko, B.-A. Li, Z.-W. Lin, and S. Pal, Phys. Rev. **C 65** (2002) 054909.
[71] D. Molnar and M. Gyulassy, Nucl. Phys. **A 697** (2002) 495.
[72] Z. Xu and C. Greiner, Elastic and inelastic multiplication collisions in a parton cascade treated in an unified manner (2004), publication in preparation.
[73] Z. Xu, PhD thesis, Universität Giessen, 2004.
[74] R. Baier, A. H. Mueller, D. Schiff, and D. T. Son. Phys. Lett. **B 502** (2001) 51.
[75] C. Greiner, S. Juchem, and Z. Xu, hep-ph/0404022.
[76] W. Cassing, K. Gallmeister, and C. Greiner. J. Phys. **G** (2004), in press.; hep-ph/0403208.
[77] K. Gallmeister, C. Greiner, and Z. Xu. Phys. Rev. **C 67** (2003) 044905.
[78] S. S. Adler *et al.*, Phys. Rev. **C 69** (2004) 034910.
[79] J. Adams *et al.*, Phys. Rev. Lett. **91** (2003) 172302.
[80] S. S. Adler *et al.*, Phys. Rev. Lett. **91** (2003) 072303.
[81] J. Adams *et al.*, Phys. Rev. Lett. **91** (2003) 072304.
[82] B. Z. Kopeliovich, J. Nemchik, E. Predazzi, and A. Hayashigaki, hep-ph/0311220.
[83] S. A. Bass *et al.*, Nucl. Phys. **A 661** (1999) 205.
[84] L. Gerland, L. Frankfurt, M. Strikman, H. Stöcker, and W. Greiner, Nucl. Phys. **A 663** (2000) 1019.
[85] C. Adler *et al.*, Phys. Rev. Lett. **87** (2001) 262302.
[86] C. Adler *et al.*, Phys. Rev. Lett. **90** (2003) 082302.
[87] D. Kharzeev, private communication.
[88] W. Schafer, H. Stöcker, B. Muller, and W. Greiner, Z. Phys. **A 288** (1978) 349.
[89] H. G. Baumgardt *et al.*, Z. Phys. **A 273** (1975) 359.
[90] D. H. Rischke, H. Stöcker, and W. Greiner, Phys. Rev. **D 42** (1990) 2283.